Supplemental Material

SUPPLEMENTAL MATERIAL FOR

Performance of pattern-scaled climate projections under high-end warming, part I: surface air temperature over land

Timothy J. Osborn[1*], Craig J. Wallace[1], Jason A. Lowe[2] and Dan Bernie[2]

[1]*Climatic Research Unit, School of Environmental Sciences, University of East Anglia, Norwich, NR4 7TJ, UK*

[2]*United Kingdom Meteorological Office Hadley Centre, Exeter, UK.*

*Corresponding author: t.osborn@uea.ac.uk

April 2018 – Revision for *Journal of Climate*

SM1. Pattern diagnosis and application of pattern scaling

This section provides a more detailed description of how patterns were diagnosed from GCM simulations and then applied to emulate GCM simulations in this study.

SM1.1 Pattern diagnosis

We follow the ClimGen approach to pattern diagnosis: a full description is given in the Supplementary Information of Osborn et al. (2016). Key points that affect the current paper are given here.

The normalised patterns (i.e. local grid-cell changes in a variable of interest per degree of global warming) for a particular GCM are diagnosed by a regression between the simulated local changes and the simulated global temperature changes. Prior to entry in the regression, both the local and global changes are smoothed with a 30-year filter to avoid the regression being dominated by signals of interannual variability such as the El Niño–Southern Oscillation. These regressions are performed separately for each grid cell on the GCM's original grid and for each of the 12 calendar months (to capture the annual cycle in the climate change signal). The slope of the regression line at each grid cell gives the normalised climate change pattern.

In principle, any simulations with forcing changes (to drive a change in global-mean temperature) could be used to diagnose that GCM's normalised response pattern. Here, we perform the regression using CMIP5 historical forcings and RCP scenario simulations combined to yield a timeseries for the period 1950–2100. For HadGEM2-ES and the other five GCMs considered here, initial-condition ensembles were available, and the simulated local and global changes were first averaged across these ensembles to strengthen the signal-to-noise ratio of the forced response to the internal variability.

The four RCP scenarios could be analysed separately, to yield four different diagnosed patterns. Alternatively, multiple RCP scenario data (pairs of values: local and global changes) can be pooled together and one regression line can be fit to the pooled, multi-RCP data pairs. The latter is the default option for the ClimGen approach, pooling data from all four RCP simulations to obtain a single normalised change pattern ("*RCPall*") for use in pattern scaling (PS). Other combinations are possible – see Table 1 for those used here. Herger et al. (2015) assess the performance of PS using patterns diagnosed from individual RCPs; it is likely that the performance using the pooled pattern *RCPall* will lie somewhere near the average of the performance of the individual patterns.

SM1.2 Application and evaluation of pattern scaling performance

To make PS projections we scaled our HadGEM2-ES *RCPall* pattern by the time evolving HadGEM2-ES RCP8.5 global-mean temperature (Fig. 1, but expressed as changes from the 1961–1990 mean level that ClimGen uses as its baseline). To evaluate the performance of the PS projection against the actual GCM data at a specific warming level of, e.g., 4°C we took the 30-year means of the PS projection and of the HadGEM2-ES data for 2052-2081 which is centred on the year when the HadGEM2-ES global-mean temperature is equal to 4°C above pre-industrial (Fig. 1). The difference between the PS and GCM 30-year means is a measure of the ability of PS to emulate the GCM response to forced warming under the RCP8.5 scenario. We have analysed these difference patterns for various months of the year and also aggregated over all land grid cells by their root-mean-squared value. The analysis is repeated for different diagnosed patterns (Table 1) and for different CMIP5 GCMs (Section SM2).

SM2. Results using additional CMIP5 GCMs

We repeated the main elements of our analysis using simulations from other CMIP5 GCMs, to supplement those presented in the main paper based on the HadGEM2-ES GCM. CMIP5 GCMs were selected using two criteria: (1) they had at least 4 initial-condition ensemble members for the historical and RCP8.5 simulations in the CMIP5 archive; and (2) climate change patterns had been diagnosed for the ClimGen PS database (Table S2 of Osborn et al. 2016). These criteria yielded five additional GCMs (Table S1).

Table S1. List of CMIP5 GCMs used in addition to HadGEM2-ES.

Model name	Reference
CanESM2	Arora et al. (2011)
CCSM4	Gent et al. (2011)
CNRM-CM5	Voldoire et al. (2013)
CSIRO-Mk3-6-0	Rotstayn et al. (2012)
IPSL-CM5A-LR	Dufresne et al. (2013)

SM2.1 Pattern-scaling performance across a range of global warming levels

A key finding from our analysis of emulating the HadGEM2-ES extended RCP simulation is that, for global warming up to 3.5°C above pre-industrial, PS using a pooled pattern closely emulates the GCM simulation but that for warming beyond 3.5°C PS performance is notably improved by using patterns diagnosed only from the high-forcing RCP8.5 scenario. A "pooled" pattern is one diagnosed by pooling GCM data across multiple simulations (Section SM1), in this case across all the available RCP simulations out to 2100.

Figure S1 to Figure S5 show equivalent results but using PS to emulate the projections from five additional CMIP5 GCMs (Table S1). These show the globally-aggregated root-mean-squared (RMS) difference between the GCM surface air temperature changes over land and the PS projections based on a pooled pattern (*RCPall*) and alternative patterns based only on RCP2.6 (*RCP26*) or RCP8.5 (*RCP85*), or a pooled pattern that excludes the RCP8.5 simulation that we are testing against (*RCP264560*, provided that an RCP6.0 simulation was available). The GCM projection that we compare against is the ensemble-mean of the first four ensemble members available, to make it comparable with the HadGEM2-ES case shown in the right-hand column of Figure 5.

Considering in particular the relative performance of PS using the *RCPall* (black) and *RCP85* (red) patterns, we see results that are mostly consistent with those found for HadGEM2-ES. In particular, the *RCPall* pattern performs slightly better than *RCP85* for specific warming levels up to ~3.5°C above pre-industrial for CanESM2 and up to ~3.0°C for CCSM4, CSIRO-Mk3-6-0 and IPSL-CM5A-LR. For CNRM-CM5, which warms the least under RCP8.5 out of the six GCMs analysed in this study, the RMS difference between the GCM and the PS projections is generally larger and shows an earlier divergence between the patterns such that PS with *RCP85* has a smaller error than with *RCPall* once global warming exceeds ~2°C (Figure S3).

SM2.2 Importance of GCM ensemble size for evaluating pattern-scaling performance

The second key finding is our quantification of the impact that internal variability has on the evaluation of PS performance, and how the apparent error is reduced by comparing against a GCM ensemble-mean and using this reduction to infer how much further the apparent error might reduce

if we had a hypothetical ensemble of infinite size (which would remove internal variability entirely). These results are shown in Figure 8 for HadGEM2-ES and can be compared with Figure S6 to Figure S10 for the other five GCMs.

For HadGEM2-ES, inferred RMS errors were less than 0.25°C for global warming levels up to ~3.5°C. Similar results are obtained for the other GCMs: inferred RMS errors are less than 0.25°C for global warming levels up to 4.0 to 4.8°C for CanESM2, to 4.0°C or more for CCSM4, 2.1 to 3.4°C for CNRM-CM5, 3.4 to 4.2°C for CSIRO-Mk3-6-0, and 4.2 to 4.7°C for IPSL-CM5A-LR. Indeed, for all GCMs except CNRM-CM5, these results are more favourable than those for HadGEM2-ES. The ranges given cover results for the four months considered (January, April, July and October).

The inferred RMS differences between PS and GCM projections grow larger than 0.25°C for global warming levels above those indicated here, but as with HadGEM2-ES, they remain small compared with the magnitude of the climate change signal and the inter-GCM spread in the CMIP5 multi-model ensemble (e.g. Herger et al., 2015; Osborn et al., 2016)

Acknowledgements. We acknowledge the World Climate Research Programme's Working Group on Coupled Modelling, which is responsible for CMIP, and we thank the climate modelling groups (listed in Table S1 of this paper) for producing and making available their model output. For CMIP the U.S. Department of Energy's Program for Climate Model Diagnosis and Intercomparison provides coordinating support and led development of software infrastructure in partnership with the Global Organization for Earth System Science Portals.

References

Arora, V. K., *et al.* (2011) Carbon emission limits required to satisfy future representative concentration pathways of greenhouse gases. *Geophys. Res. Lett.* **38**, L05805. doi: 10.1029/2010GL046270

Dufresne, J.-L., *et al.* (2013) Climate change projections using the IPSL-CM5 Earth System model: from CMIP3 to CMIP5. *Clim. Dyn.* **40**, 2123–2165. doi: 10.1007/s00382-012-1636-1

Gent, P. R., *et al.* (2011) The Community Climate System Model Version 4. *J. Climate* **24**, 4973–4991, https://doi.org/10.1175/2011JCLI4083.1

Herger, N., Sanderson, B. M., and Knutti, R. (2015) Improved pattern scaling approaches for the use in climate impact studies. *Geophys. Res. Lett.* **42**, 3486–3494. doi: 10.1002/2015GL063569

Osborn, T. J., Wallace, C. J., Harris, I. C. and Melvin, T. M. (2016). Pattern scaling using ClimGen: monthly-resolution future climate scenarios including changes in the variability of precipitation. *Climatic Change* **134**, 353–369. http://doi.org/10.1007/s10584-015-1509-9

Rotstayn, L. D., *et al.* (2012) Aerosol- and greenhouse gas-induced changes in summer rainfall and circulation in the Australasian region: a study using single-forcing climate simulations. *Atmos. Chem. Phys.* **12**, 6377–6404. https://doi.org/10.5194/acp-12-6377-2012

Voldoire, A., *et al.* (2013) The CNRM-CM5.1 global climate model: description and basic evaluation. *Clim. Dyn*. **40**, 2091–2121. https://doi.org/10.1007/s00382-011-1259-y

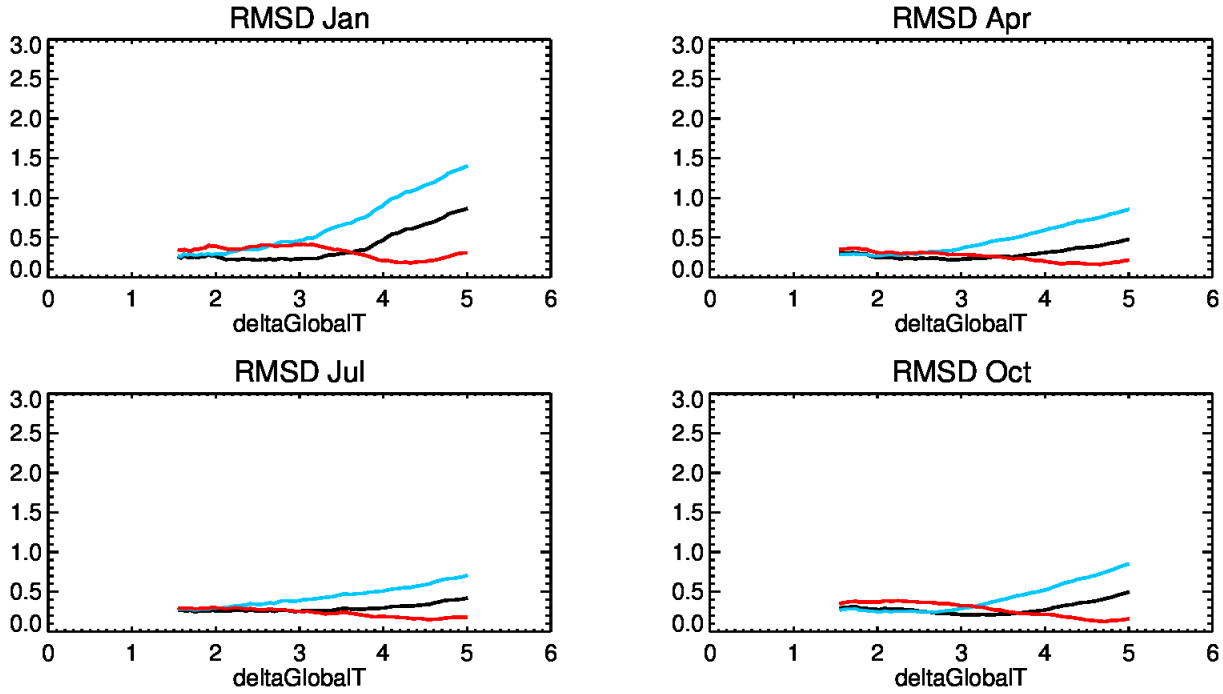

Figure S1. Similar to the right-hand column of Fig. 5 of the main paper, but for the CanESM2 GCM. Global land RMS difference (°C), as a function of ΔT, between gridded PS projections (using patterns RCPall, black; RCP26, blue; and RCP85, red) and the ensemble-mean GCM projection (2001–2100, right column). Results are shown separately for January, April, July and October.

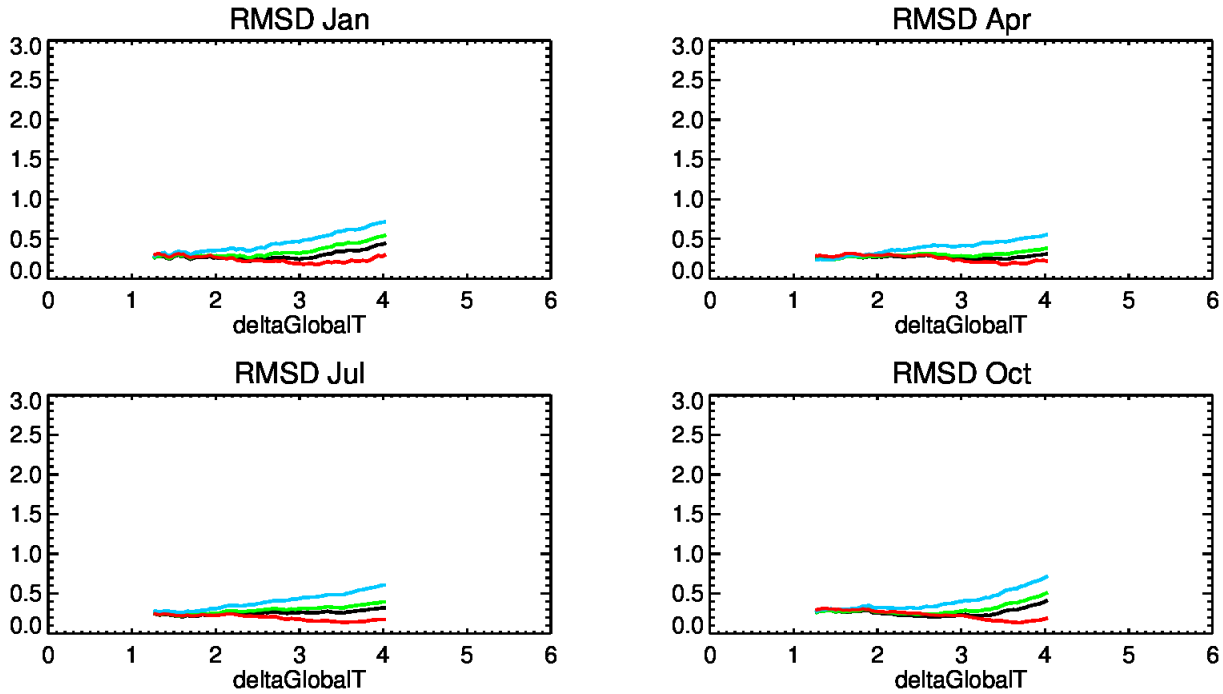

Figure S2. Similar to the right-hand column of Fig. 5 of the main paper, but for the CCSM4 GCM. The green line is for PS projections using the RCP264560 pattern.

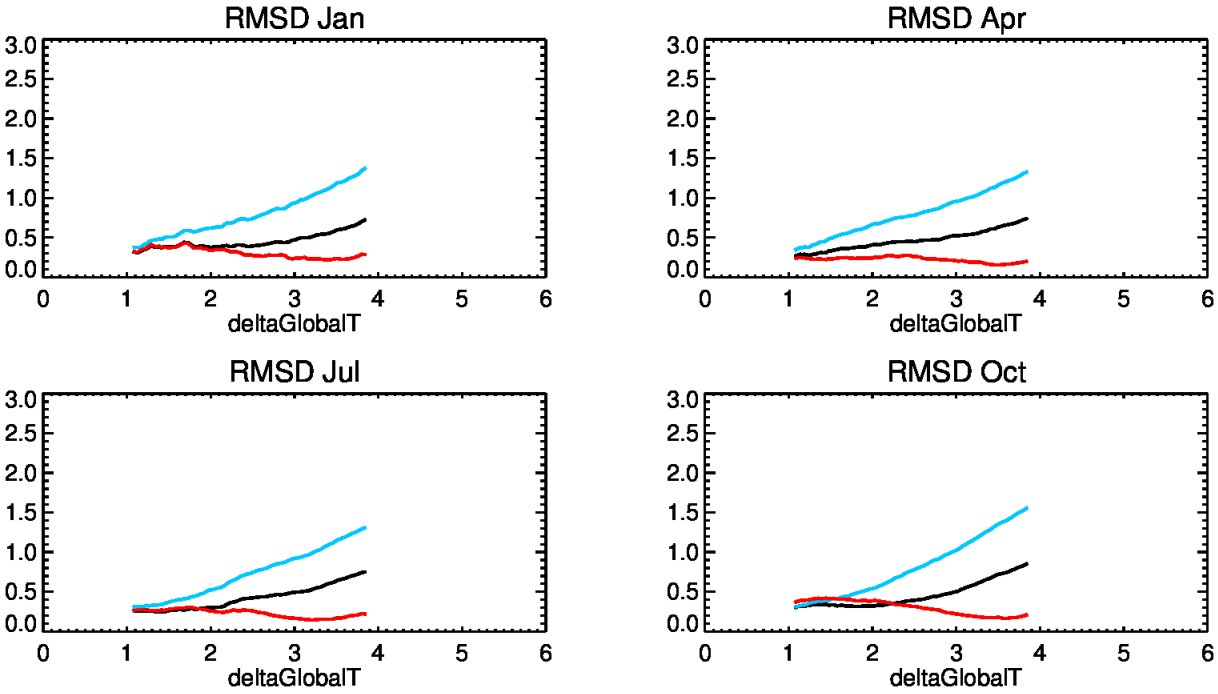

Figure S3. Similar to the right-hand column of Fig. 5 of the main paper, but for the CNRM-CM5 GCM.

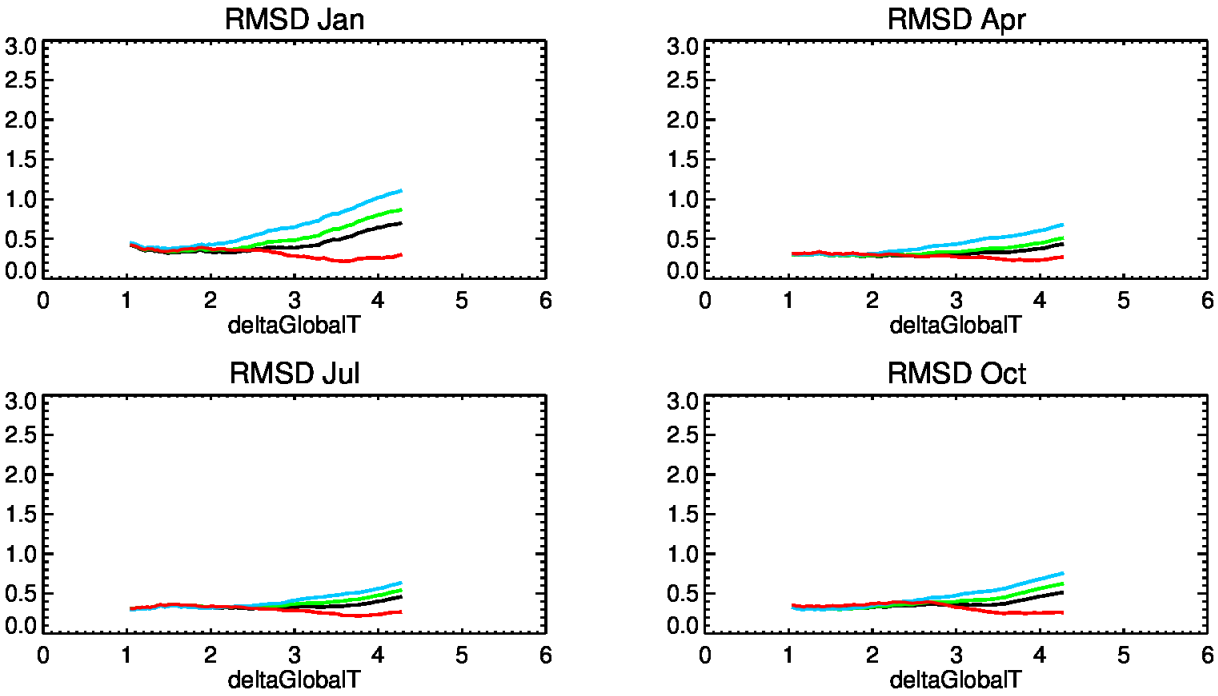

Figure S4. Similar to the right-hand column of Fig. 5 of the main paper, but for the CSIRO-Mk3-6-0 GCM.

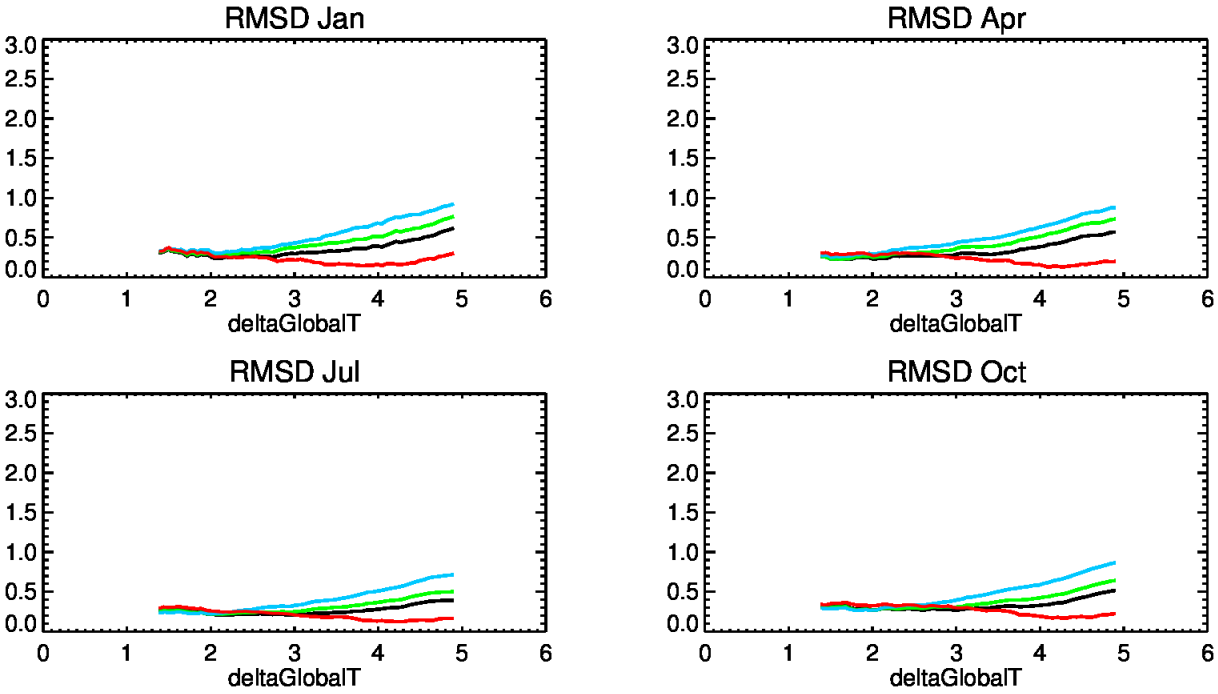

Figure S5. Similar to the right-hand column of Fig. 5 of the main paper, but for the IPSL-CM5A-LR GCM.

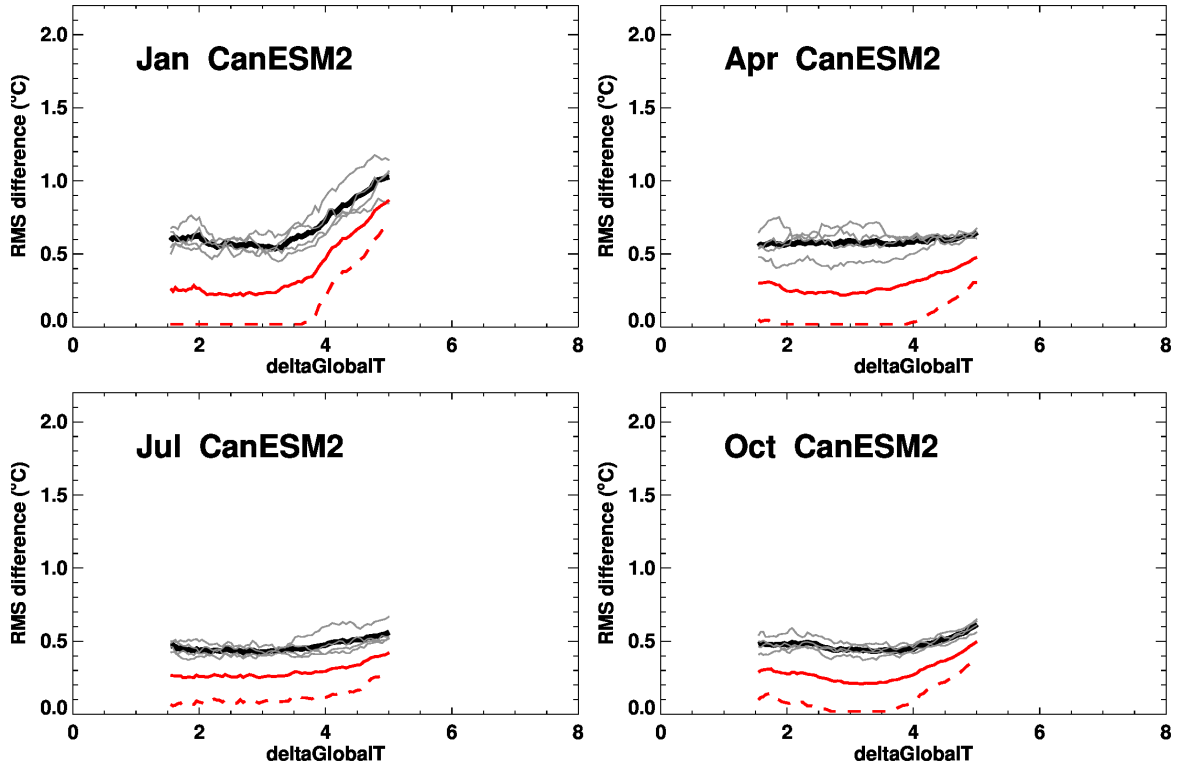

Figure S6. Similar to Fig. 8 of the main paper, but for the CanESM2 GCM. Global land RMS differences (°C) between gridded PS projections (RCPall) and each single-member GCM RCP8.5 projection (grey) and the ensemble-mean GCM projection (red), under RCP8.5, as a function of ΔT. The mean of the individual ensemble member results is shown in black, and the red dashed line indicates the inferred RMS difference from a hypothetical infinite ensemble. Results shown separately for January, April, July and October.

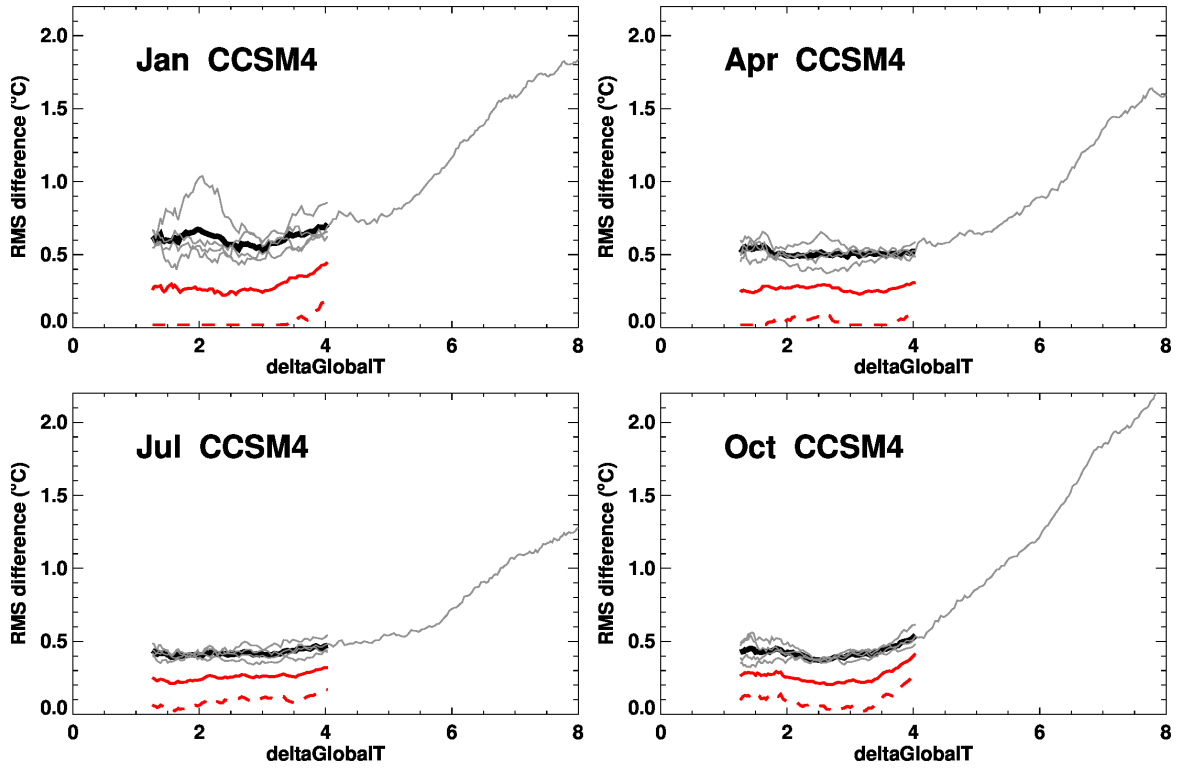

Figure S7. Similar to Fig. 8 of the main paper, but for the CCSM4 GCM.

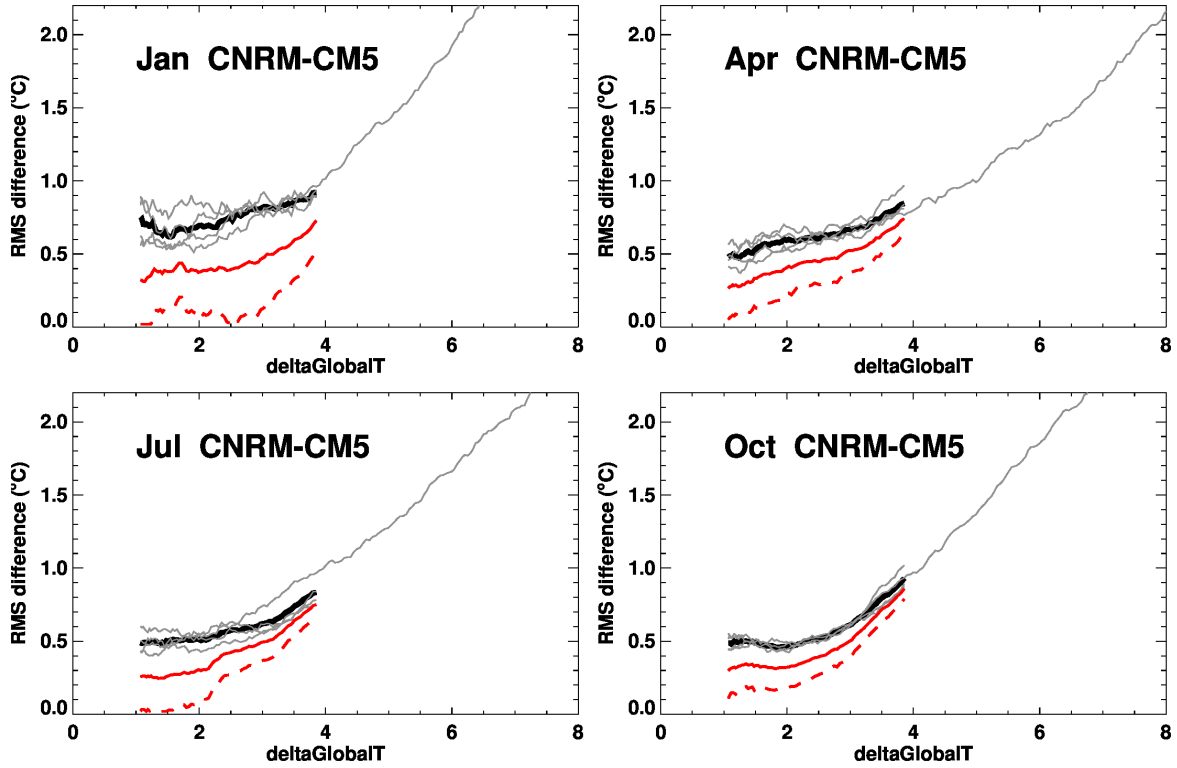

Figure S8. Similar to Fig. 8 of the main paper, but for the CNRM-CM5 GCM.

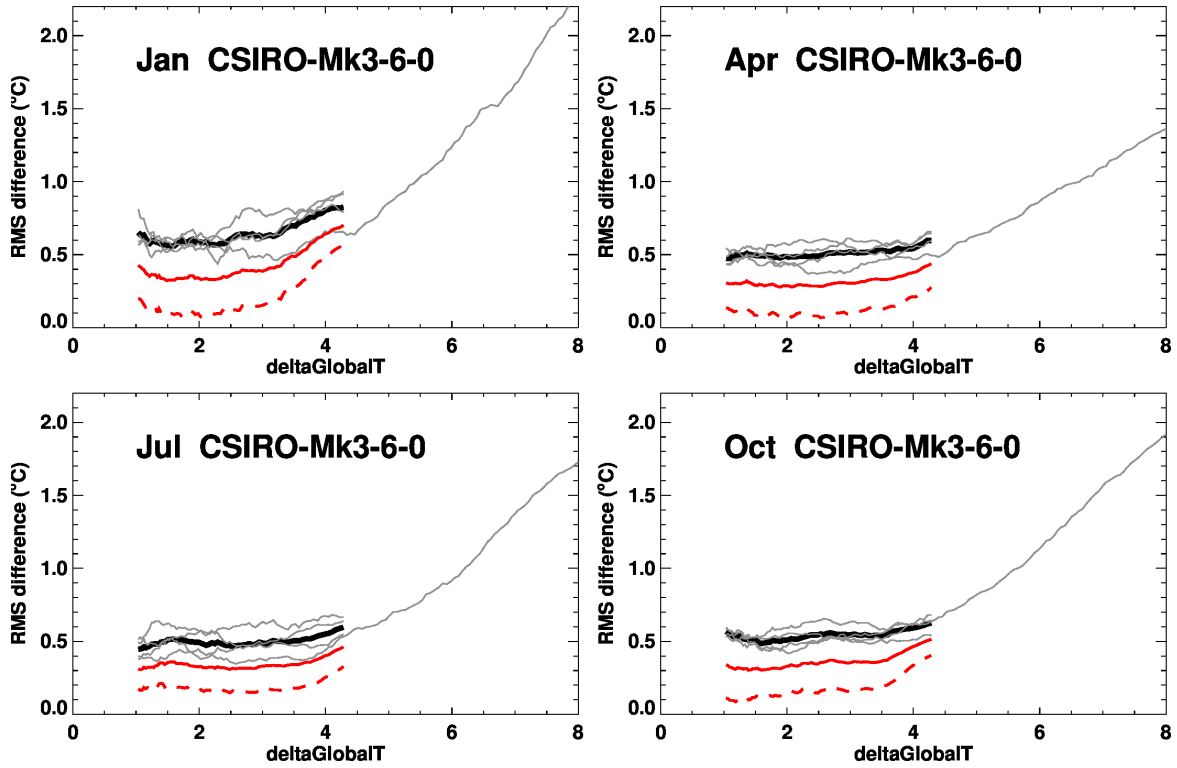

Figure S9. Similar to Fig. 8 of the main paper, but for the CSIRO-Mk3-6-0 GCM.

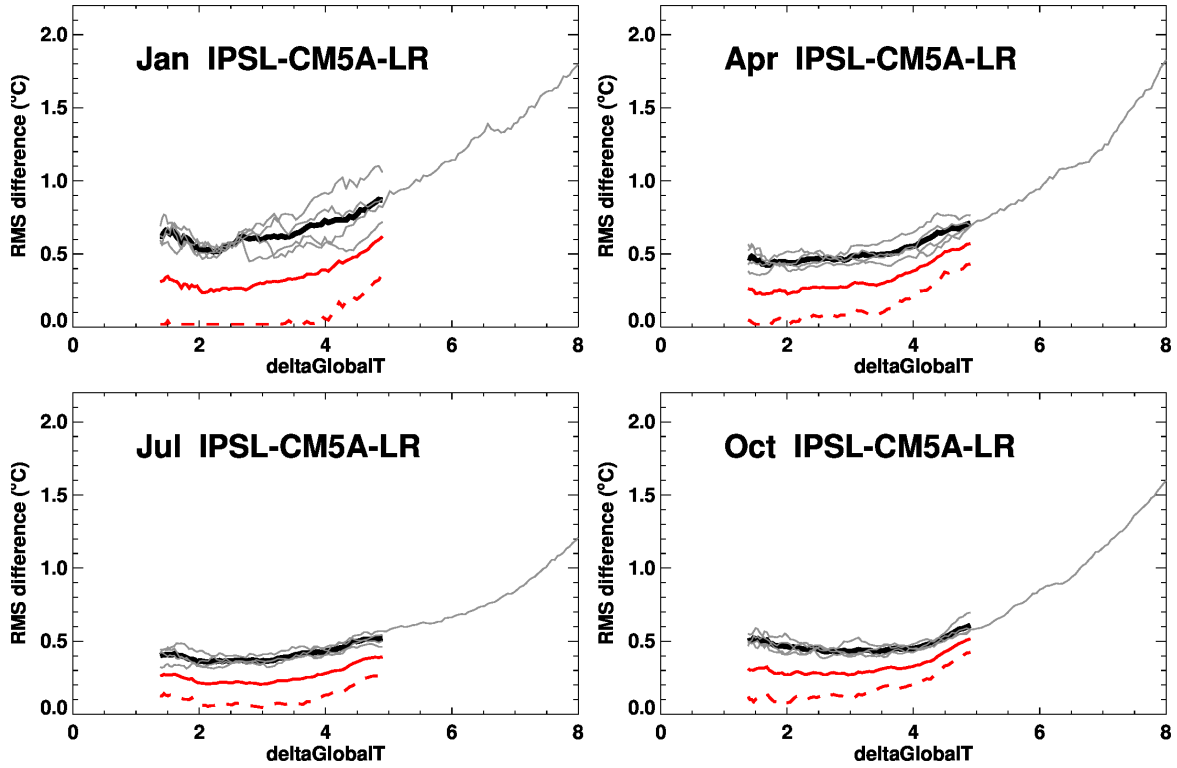

Figure S10. Similar to Fig. 8 of the main paper, but for the IPSL-CM5A-LR GCM.